



HAL
open science

VUV photochemistry of cyclopropenone ($c\text{-C}_3\text{H}_2\text{O}$): formation rate and abundance ratios of propynal (HCCCHO) and propadienone ($\text{CH}_2\text{>CCO}$)

Mohamad Ibrahim, Jean-claude Guillemin, Lahouari Krim

► **To cite this version:**

Mohamad Ibrahim, Jean-claude Guillemin, Lahouari Krim. VUV photochemistry of cyclopropenone ($c\text{-C}_3\text{H}_2\text{O}$): formation rate and abundance ratios of propynal (HCCCHO) and propadienone ($\text{CH}_2\text{>CCO}$). Physical Chemistry Chemical Physics, In press, 10.1039/D4CP03895A . hal-04870428

HAL Id: hal-04870428

<https://hal.science/hal-04870428v1>

Submitted on 7 Jan 2025

HAL is a multi-disciplinary open access archive for the deposit and dissemination of scientific research documents, whether they are published or not. The documents may come from teaching and research institutions in France or abroad, or from public or private research centers.

L'archive ouverte pluridisciplinaire **HAL**, est destinée au dépôt et à la diffusion de documents scientifiques de niveau recherche, publiés ou non, émanant des établissements d'enseignement et de recherche français ou étrangers, des laboratoires publics ou privés.

VUV photochemistry of cyclopropenone (c-C₃H₂O): formation rate and abundance ratios of propynal (HCCCHO) and propadienone (CH₂CCO)

Mohamad Ibrahim¹, Jean-Claude Guillemin² and Lahouari Krim^{1*}

¹*Sorbonne Université, CNRS, De la Molécule aux Nano-Objets: Réactivité, Interactions, Spectroscopies, MONARIS, 75005, Paris, France.*

²*Univ Rennes, Ecole Nationale Supérieure de Chimie de Rennes, CNRS, ISCR – UMR6226, F-35000 Rennes, France.*

* *Corresponding author: Lahouari.krim@Sorbonne-universite.fr*

Abstract

The distribution of isomeric species in the interstellar medium cannot be directly related to their relative energetic stabilities, but more to their mechanisms of formation and evolution. The abundances of the three isomers of C₃H₂O, cyclopropenone, propynal and propadienone show an example among many other interstellar species where kinetic effects would control their presence in astrophysical regions. Until today, only propynal and cyclopropenone, the two less stable isomers of propadienone have been detected in the interstellar medium. In this work, we have examined the vacuum ultraviolet (VUV) photochemistry of cyclopropenone (c-C₃H₂O), an unsaturated ketone and aromatic compound which is the thermodynamically most unstable form of the three isomers of C₃H₂O. Using Fourier transform infrared spectroscopy and mass spectrometry to probe the photoproducts, we have investigated the photolysis of cyclopropenone ice and cyclopropenone trapped in neon matrix. We show that the VUV photolysis of c-C₃H₂O ice at 10 K leads mainly to CO and C₂H₂ fragments, in addition to propynal HCCCHO and propadienone CH₂CCO. The distribution of the two isomers depends on the irradiation time. At short irradiation time, HCCCHO is formed with twice the abundance of the most stable isomer CH₂CCO, while by increasing the irradiation time, the same abundance are observed showing that equilibrium is reached between the two isomers. The photolysis of c-C₃H₂O isolated in neon matrix has allowed the characterization of HCCCO and CCCO as reaction intermediates, resulting from VUV-induced dehydrogenation of cyclopropenone, and which are the precursors of propynal and propadienone through CCCO + 2H reaction.

Introduction

Cyclopropenone ($c\text{-C}_3\text{H}_2\text{O}$) is one of the smallest aromatic molecules¹ which has been detected in a variety of objects of the interstellar medium. $c\text{-C}_3\text{H}_2\text{O}$ has been first observed in Sagittarius B2 with fractional abundances² of about 6×10^{-11} , and was later found in the cold dense molecular³ cloud L1527. The most recent radio-astronomical study⁴ led to the identification of cyclopropenone in four dark clouds or prestellar cores TMC-1, B1-b, L483 and Lupus-1A. Formation routes of cyclopropenone have been the subject of several experimental and theoretical studies. Petrie et al⁵ proposed that the reaction between OH and cyclopropenylidene ($c\text{-C}_3\text{H}_2$) leads to cyclopropenone. Recently, using the DFT calculations, Loison et al⁴ showed that this reaction proceeds without energy barriers. In addition, Ahmadvand et al⁶ proposed three possible reaction mechanisms of cyclopropenone in ISM, the first reaction proposed is between atomic oxygen and $c\text{-C}_3\text{H}_2$, the second one between O_2 and $c\text{-C}_3\text{H}_2$, and the third possible reaction between carbon monoxide and acetylene. They show that the $\text{O}_2 + c\text{-C}_3\text{H}_2$ reaction may occur without energy barriers and represents a likely reaction pathway to synthesize interstellar $c\text{-C}_3\text{H}_2\text{O}$. In contrast, the $\text{CO} + \text{C}_2\text{H}_2$ reaction has a very high energy barrier and is therefore unfavorable at low temperature. Related to experimental studies, more than a decade of laboratory astrochemistry studies on interstellar ice analogues have permitted to propose formation mechanisms for cyclopropenone under conditions of the interstellar medium. Despite the high barrier for the $\text{CO} + \text{C}_2\text{H}_2$ reaction, Zhou et al⁷ investigated the formation of $\text{C}_3\text{H}_2\text{O}$ isomers by irradiating $\text{CO}\text{-C}_2\text{H}_2$ ices with 5 keV electrons. J. Wang et al⁸. confirmed the formation of propynal, cyclopropenone, and propadienone through UV photolysis of $\text{CO}\text{-C}_2\text{H}_2$ ices using low photon energies ranged between 4.3 and 5.6 eV. Additionally, a matrix isolation study has been carried out to investigate the formation of $\text{C}_3\text{H}_2\text{O}$ isomers. In this context, Zaslavskiy et al^{9,10} have shown that 20 keV X-ray irradiation of C_2H_2 and CO isolated in rare-gas matrices (Ar, Kr, and Xe) leads to the formation of the three isomers of $\text{C}_3\text{H}_2\text{O}$: cyclopropenone, propynal and propadienone. Very few experimental studies have been carried out with cyclopropenone. The only previous studies on the UV photolysis (250-350 nm) of cyclopropenone have been carried out in aqueous and methanolic solutions to investigate $c\text{-C}_3\text{H}_2\text{O}$ decarbonylation, which leads to C_2H_2 and CO as photo-products^{11,12}. Furthermore, the photoelectron spectra of cyclopropenone have been investigated by Harshbarger et al¹³. They show that the first ionization potential is located at 9.57 eV and involves ionization of the oxygen atom, while the two other ionization potentials involving the C=O bond and the second lone pair orbital of

oxygen are located at 11.19 and 16.11 eV, respectively. Recently, our group¹⁴ has investigated the hydrogenation reaction of cyclopropenone ice at 10 K, showing that the $c\text{-C}_3\text{H}_2\text{O} + \text{H}$ solid state reaction leads to propynal (HCCCHO) and propadienone (CH_2CCO), the most stable isomers of cyclopropenone, in addition to hydrogenated species namely: propenal (CH_2CHCHO), propanal ($\text{CH}_3\text{CH}_2\text{CHO}$), $c\text{-C}_3\text{H}_4\text{O}$ (cyclopropanone), cyclopropanol ($c\text{-C}_3\text{H}_6\text{O}$) and propanol ($\text{CH}_3\text{CH}_2\text{CH}_2\text{OH}$).

The present work focuses on the photochemistry in solid phase at 10 K of the less stable isomer of $\text{C}_3\text{H}_2\text{O}$, in two different environments: $c\text{-C}_3\text{H}_2\text{O}$ ice (dense phase) and $c\text{-C}_3\text{H}_2\text{O}$ trapped in neon matrix (diluted phase), at two different irradiation times. At short time irradiation the processes involved are dominated by the photodecomposition of cyclopropenone, as the main reactant. At long irradiation time the abundances of final photoproducts result from reactions due to the photolysis of both $c\text{-C}_3\text{H}_2\text{O}$ and the primary photoproducts. This study focuses in how $c\text{-C}_3\text{H}_2\text{O}$, already detected in the interstellar medium may evolve through energetic processing and what are the reaction mechanisms involved in its transformation.

Experimental setup

The experimental set-up used in this study has been described in previous articles¹⁵, thus a few specific details are mentioned hereafter. The experiments are performed under ultra high vacuum at 10^{-10} mbar. Samples are condensed onto a cryogenic mirror maintained at low temperature, using a pulsed tube closed-cycle cryogenerator (Sumitomo cryogenics F-70). Using a Bruker 120 FTIR spectrometer, our solid samples are spectrally characterized by recording infrared spectra in the transmission reflection mode between 5000 and 500 cm^{-1} , with a resolution of 0.5 cm^{-1} . Cyclopropenone ($c\text{-C}_3\text{H}_2\text{O}$) has been synthesized as previously reported¹⁶ and stored under vacuum in a reservoir at -196°C in liquid nitrogen. $c\text{-C}_3\text{H}_2\text{O}$ liquid is partially evaporated at 10°C and injected into the experimental chamber, pure or mixed with neon gas. The solid samples are then irradiated at low temperature using a vacuum ultraviolet (VUV) light source (Hamamatsu L10706 UV) with a total flux of 10^{15} photons $\text{cm}^{-2}\text{ s}^{-1}$. The lamp has a broad light spectrum with a spectral distribution between 115 and 400 nm, with the main emission peak at 160 nm (7.7 eV) and a small additional peak at 125 nm (9.9 eV). The photolysis of the $c\text{-C}_3\text{H}_2\text{O}$ has been carried out using two different experimental methods:

- Method 1: Photolysis in dense phase at 10 K

This experiment consists of the formation of $c\text{-C}_3\text{H}_2\text{O}$ ice by condensing $c\text{-C}_3\text{H}_2\text{O}$ gas on the cryogenic mirror maintained at 10 K. The resulting ice is then irradiated at 10 K during two different time scales: 2 and 30 min.

- Method 2: Photolysis in diluted phase at 3 K

This second experiment consists of isolating $c\text{-C}_3\text{H}_2\text{O}$ in a neon matrix at 3K. The sample is prepared by condensing $c\text{-C}_3\text{H}_2\text{O}/\text{Ne} = 1/100$ mixtures onto the cryogenic mirror maintained at 3K. Just after photolysis during 30 min, the irradiated matrix is heated from 3 to 20 K, to remove the neon atoms, and cooled down to 10 K to recover an irradiated $c\text{-C}_3\text{H}_2\text{O}$ ice, which can be compared to $c\text{-C}_3\text{H}_2\text{O}$ ice irradiated at 10 K performed with the first experimental method.

For the two experimental methods, the solid samples are characterized before and after irradiation using IR spectroscopy. In order to complete the infrared the spectral assignment carried out in solid phase, we have also investigated Temperature Programmed Desorption (TPD) using a quadrupole mass spectrometer (QMS—Hidden Analytical) detection. Irradiated and non-irradiated $c\text{-C}_3\text{H}_2\text{O}$ ices are then heated progressively from 10 to 300 K to characterize the reactants and photoproducts released into the gas phase.

Results

Photolysis of $c\text{-C}_3\text{H}_2\text{O}$: Infrared spectroscopy analysis

Figure 1a illustrates the IR spectrum in the mid infrared spectral region of $c\text{-C}_3\text{H}_2\text{O}$ ice formed at 10 K. The most characteristic IR signals of cyclopropanone are located at 1849 and 1783 cm^{-1} corresponding to ν_2 and $2\nu_{11}$ vibrational modes, respectively. The assignments of the most important vibrational absorption band of $c\text{-C}_3\text{H}_2\text{O}$ ice, namely C=O, C=C, C-H and C-C stretching modes, CH wagging modes, deduced from experimental¹⁷ and theoretical¹⁸ studies are listed in table 1.

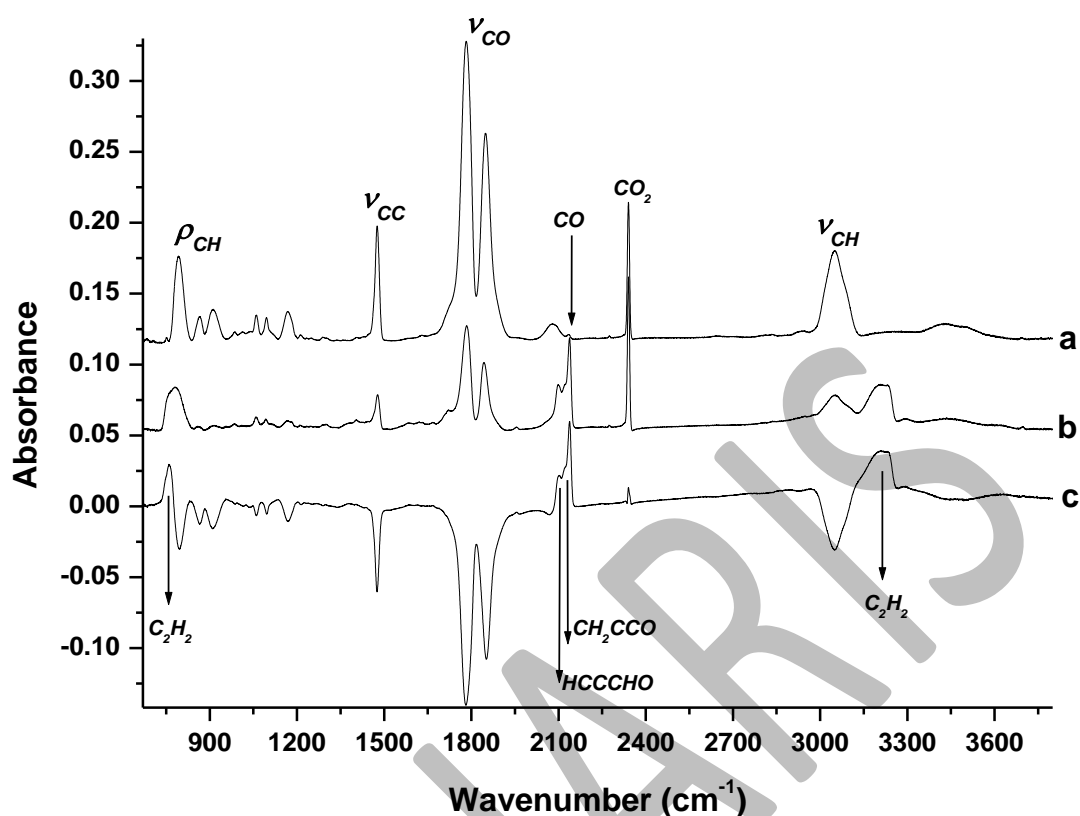


Figure 1. IR spectrum of cyclopropenone ($c\text{-C}_3\text{H}_2\text{O}$) ice formed at 10 K (a) before VUV-irradiation, (b) after VUV-irradiation. (c) Difference spectrum before and after VUV-irradiation of $c\text{-C}_3\text{H}_2\text{O}$ ice.

Figure 1b shows the IR spectrum of $c\text{-C}_3\text{H}_2\text{O}$ ice after 30 min VUV irradiation. Figure 1c represents the difference spectrum, before and after ice photolysis, where the negative and positive IR signals correspond to the reactant consumed and photoproducts formed during 30 min photolysis, respectively. Under such experimental conditions, 65% of cyclopropenone is consumed to form several photoproducts with main IR absorption signals at 3240, 2138, 2125, 2097 and 758 cm^{-1} , in addition to weak signals or signals overlapping with the absorption bands of $c\text{-C}_3\text{H}_2\text{O}$ around 2234, 2250, 1666 and 952 cm^{-1} . These weak signals will be re-examined in figure 3b and discussed with the results of the second experimental method which allow reducing the spectral overlap between the IR signals of the photoproducts and those of $c\text{-C}_3\text{H}_2\text{O}$ reactant. All or parts of these IR signals have already been observed by different groups interested into the formation of cyclopropenone and their isomers^{7,8}, or in the infrared characterization of pure ices^{14,18-22} namely, CO, C_2H_2 , $c\text{-C}_3\text{H}_2\text{O}$ and HCCCHO. Based on the comparison between data from the literature and our experimental observations, table 1 gathers the main photoproducts resulting from the VUV photolysis of $c\text{-C}_3\text{H}_2\text{O}$ ice.

We show that 30 min VUV irradiation of $c\text{-C}_3\text{H}_2\text{O}$ ice leads to C_2H_2 , CO , C_3O , HCCCHO and CH_2CCO as main photoproducts.

Table 1. Infrared absorption bands of pure $c\text{-C}_3\text{H}_2\text{O}$ ice formed at 10K and Spectral positions (cm^{-1}) of the main reaction products resulting from VUV photolysis of $c\text{-C}_3\text{H}_2\text{O}$ ice.

IR signal before VUV photolysis (cm^{-1})	$c\text{-C}_3\text{H}_2\text{O}$ vibrational modes ^{13,14}	IR signal After VUV photolysis (cm^{-1})	Literature ^{7,8,19-22}	Reaction products
		3287	3234	HCCCHO
		3240	3240	C_2H_2
3090	ν_1 C-H str.			
3052	ν_9 C-H str.			
		2250	2250	CCCO
		2138	2138	CO
		2125	2125	CH_2CCO
		2097	2099	HCCCHO
1849	ν_2 C=O str.			
1783	$2\nu_{11}$ overtone			
		1665	1666	HCCCHO
1476	ν_3 C=C str.			
1168	ν_{10} C-C str.			
		957	952	HCCCHO
909	ν_{11} C-H wag (in-plane)			
864	ν_5 C-H wag (in-plane)			
792	ν_7 C-H wag (out-of-plane)			
		758	742	C_2H_2

The same experiment has been performed by reducing the irradiation time from 30 to 2 min. After 2 min VUV photolysis of $c\text{-C}_3\text{H}_2\text{O}$ ice, the same photoproducts are formed in small amounts, however, CO , C_2H_2 , HCCCHO and CH_2CCO photoproducts have different

abundances from those obtained after 30 min VUV irradiation. Figure 2 shows the difference spectrum after and before ice photolysis for the 30 and 2 min irradiations.

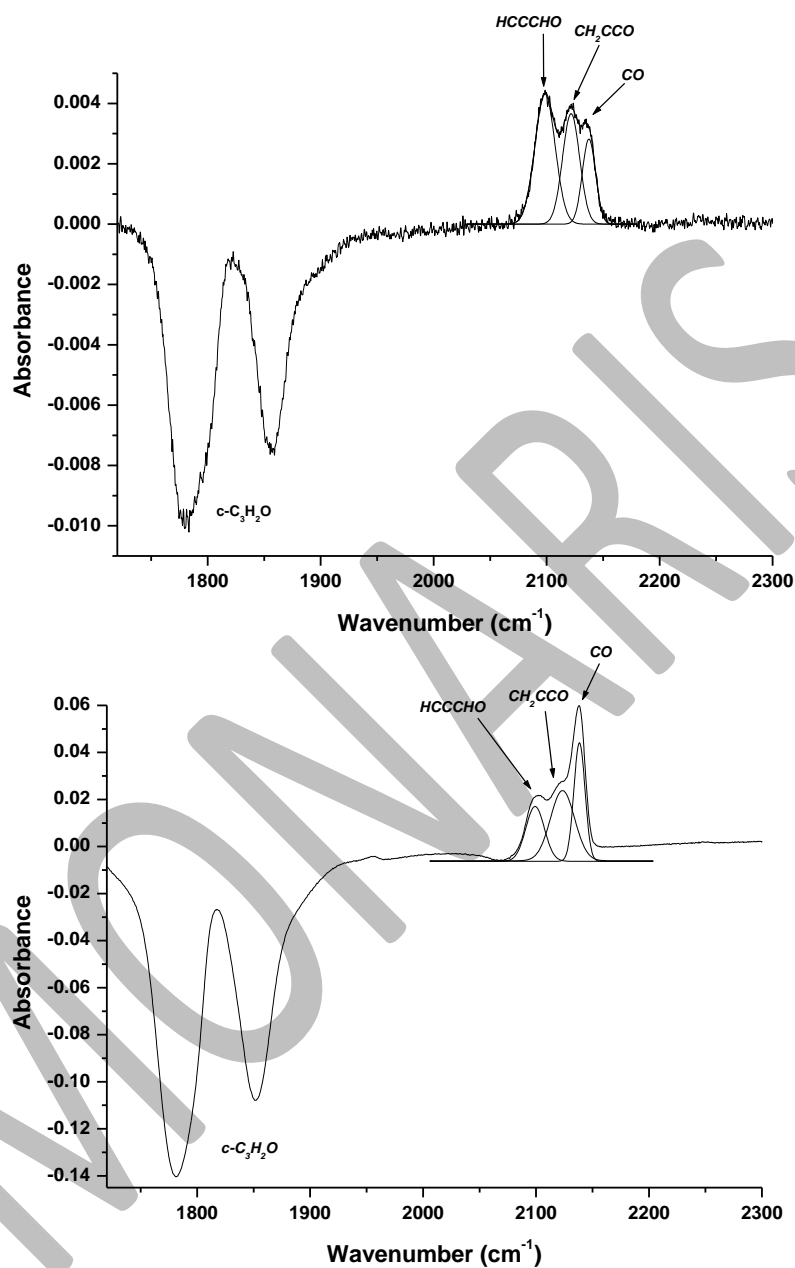


Figure 2: Difference spectrum after and before VUV-irradiation of $c\text{-C}_3\text{H}_2\text{O}$ ice with two different irradiation times: up) 2 min, down) 30 min.

From figure 2, we note that by reducing the irradiation time from 30 to 2 min, we reduce the abundances of photoproducts and also the consumption of $c\text{-C}_3\text{H}_2\text{O}$. However at short irradiation time the production of propynal seems to be more favorable than that of propadienone. In order to have the distribution of the photoproducts for the two irradiation

times (2 and 30 min), we have calculated $c\text{-C}_3\text{H}_2\text{O}$, HCCCHO, CH_2CCO , CO and C_2H_2 column densities \mathbf{n} (molecule cm^{-2}), using the IR integrated intensities as:

$$\mathbf{n} = \frac{\ln 10 \int I(\nu) \cos(8^\circ)}{\mathbf{A} \cdot 2}$$

$\int I(\nu)$ and \mathbf{A} are the integrated absorption band and IR band strength, respectively. $\cos(8^\circ)/2$ is a correction term taking into account the geometry of our IR measurements²³. Table 2 lists the spectral positions of the vibrational modes considered for our column densities calculations and their corresponding band strengths. It also gathers the column densities for the $c\text{-C}_3\text{H}_2\text{O}$ consumed and those of photoproducts formed during the two different irradiation times.

Table 2: Column densities of reactant consumed ($c\text{-C}_3\text{H}_2\text{O}$) and products formed (CO and C_2H_2 fragments, HCCCHO and CH_2CCO isomers) during the VUV irradiation of $c\text{-C}_3\text{H}_2\text{O}$ ice.

	Reactant consumed ^b	Photoproducts formed			
		Photofragments		Isomers	
	$c\text{-C}_3\text{H}_2\text{O}$	CO	C_2H_2	Propadienone	Propynal
Position (cm^{-1})	1849	2138	758	2125	2097
$\mathbf{A}^a(\text{cm molecule}^{-1})$	28.0×10^{-18}	8.7×10^{-18}	24.2×10^{-18}	28.0×10^{-18}	18.2×10^{-18}
After 2 min irradiation					
$\mathbf{n}(\text{molecule cm}^{-2})$	-1.6×10^{16}	5.4×10^{15}	2.4×10^{15}	2.8×10^{15}	6.1×10^{15}
After 30 min irradiation					
$\mathbf{n}(\text{molecule cm}^{-2})$	-21.7×10^{16}	81.2×10^{15}	33.9×10^{15}	32.5×10^{15}	29.9×10^{15}

a) The infrared band strengths are taken from references 20 (for C_2H_2), 22 (for $c\text{-C}_3\text{H}_2\text{O}$, CH_2CCO and HCCCHO), 24 (for CO).

b) Negative column density values correspond to the amount of $c\text{-C}_3\text{H}_2\text{O}$ consumed during the photolysis.

From table 2, we notice that after 2 min irradiation 1.60×10^{16} molecule. cm^{-2} are consumed to form 1.67×10^{16} molecules. cm^{-2} of photoproducts, while, by increasing the ice irradiation time to 30 min, the consumption of 21.7×10^{16} molecule. cm^{-2} of reactants leads only to 17.8×10^{16} molecule. cm^{-2} of photoproducts. This observed difference between the quantities of molecules produced and consumed becomes significant in the case of long-term irradiation. It shows that

other processes, such as mass loss by diffusion or evaporation, must be taken into account in molecular consumption during photolysis.

We have calculated the CO:C₂H₂:CH₂CCO:HCCCHO column density distribution after 2 and 30 min of ice irradiation. After 2 min irradiation of c-C₃H₂O ice at 10 K, CO, C₂H₂, CH₂CCO, HCCCHO are formed with a column density distribution CO:C₂H₂:CH₂CCO:HCCCHO = 1:0.4:0.5:1, where the two isomers CH₂CCO and HCCCHO are detected with two different abundances. It should be noted that with a short irradiation time, the production of the less stable HCCCHO isomer is twice as high as that of the thermodynamically more stable CH₂CCO isomer. While after 30 min irradiation, the CO:C₂H₂:CH₂CCO:HCCCHO column density distribution is equal to 1:0.4:0.4:0.4, showing that both CH₂CCO and HCCCHO are produced with the same abundances. These results underline the kinetic effect on the abundance distribution of the photoproducts resulting from photolysis of interstellar ice analogs.

In addition to the effects of the irradiation time on the photolysis of c-C₃H₂O ice, we have also investigated the role of the environment by studying the photo-induced reaction of c-C₃H₂O isolated in neon matrix at 3K. The photolysis in diluted phase at 3 K consists in the preparation of neon matrix where c-C₃H₂O is trapped in a neutral cage by co-condensing c-C₃H₂O/Ne = 1/100 on a substrate maintained at 3 K. After 30 min photolysis, the irradiated matrix is heated from 3 to 20 K, to remove the neon atoms, and cooled down to 10 K to recover an irradiated c-C₃H₂O ice, the results of which can be compared to those obtained with the direct irradiation of c-C₃H₂O ice at 10 K. The results of the photolysis in diluted phase are presented in figure 3b, where the IR spectrum is recorded at 10 K after 30 min irradiation and after removing neon atoms from the sample.

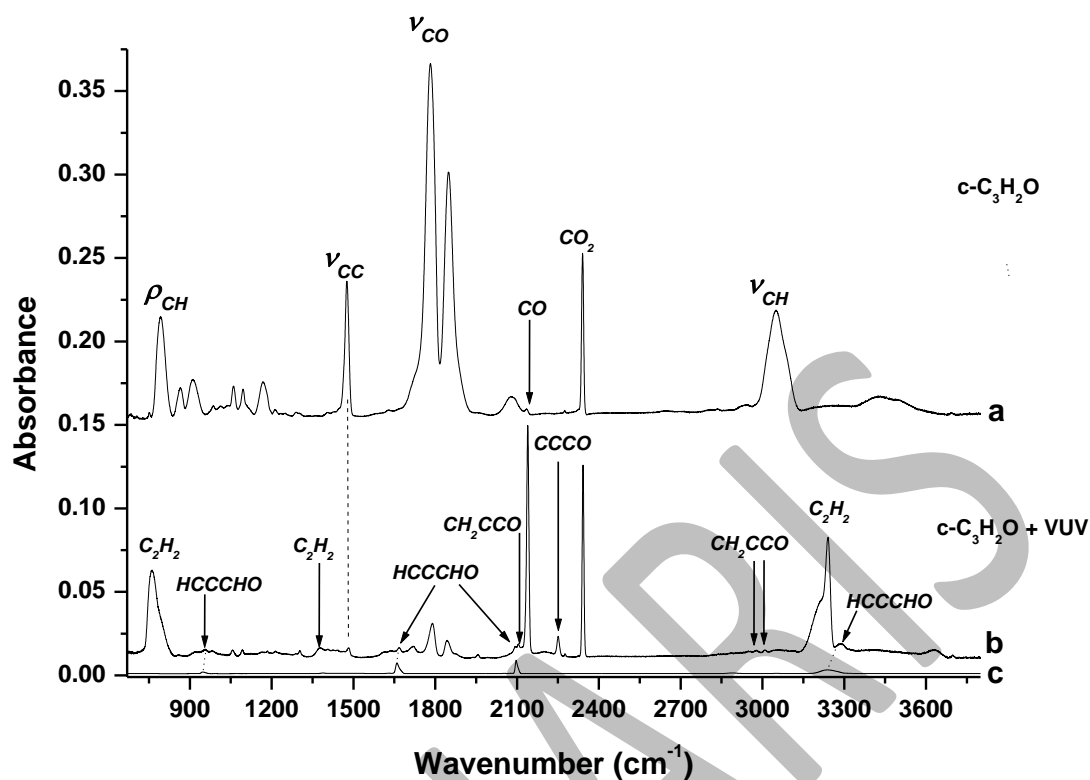


Figure 3: (a) IR spectrum of cyclopropenone ($c\text{-C}_3\text{H}_2\text{O}$) ice formed at 10 K. (b) after VUV irradiation of $c\text{-C}_3\text{H}_2\text{O}$ isolated in Ne matrix at 3 K followed by a total sublimation of neon atoms at 20 K, then a cooling down to 10 K to recover an irradiated $c\text{-C}_3\text{H}_2\text{O}$ ice. (c) IR spectrum of propynal ice recorded, to be compared to the IR signatures of photoproducts.

As a reference, figure 3a shows the IR spectrum of cyclopropenone ($c\text{-C}_3\text{H}_2\text{O}$) ice formed at 10 K in order to distinguish the IR signals of the photoproducts from those of the reactant. Similarly, we have also recorded the IR spectrum of propynal ice to be compared to the IR signatures of photoproducts. Figure 3b shows that all the reaction products formed during the photolysis of $c\text{-C}_3\text{H}_2\text{O}$ ice at 10 K and discussed above, are also detected during the photolysis of $c\text{-C}_3\text{H}_2\text{O}$ in diluted phase. As mentioned earlier, with such an experiment and compared to figure 1b, the IR signals of the photoproducts are more visible, as those of the reactant are almost vanished (see ν_{CC} and ν_{CO} of $c\text{-C}_3\text{H}_2\text{O}$ in figure 1b versus figure 3b). This allows a better characterization of the two isomers propynal and propadienone in different spectral regions and those of the photo fragments CO and C_2H_2 . However, using this experimental method, tricarbon monoxide CCCO is clearly observed as a reaction product at 2250 cm^{-1} , even after neon atom desorption, showing a total dehydrogenation of cyclopropenone. CCCO has been already detected through IR observations at 2250 cm^{-1} by

several groups investigating the processing of CO-C₂H₂ ice mixtures of by energetic sources^{7,8}. In addition to CCCO, we have also detected²⁵ at 2320 cm⁻¹ HCCCO which disappears during the sublimation of neon matrix at 20 K. Figure 4 shows, in the CCCO and HCCCO infrared spectral region, the IR spectrum of cyclopropenone isolated in neon matrix at 3 K before and after matrix photolysis. After VUV irradiation (figure 4b), two signals appear at 2253 and 2320 cm⁻¹ which can be assigned to CCCO and HCCCO photoproducts^{9,25}, respectively. Figure 4c shows the results obtained after matrix photolysis followed by total sublimation of neon atoms at 20 K, then a cooling down to 10 K to recover an irradiated c-C₃H₂O ice. We notice that the IR signal corresponding to HCCCO disappears while that of CCCO decreases and shifts to 2250 cm⁻¹. The intensity of the integrated CCCO band is 0.2 cm⁻¹ at 3K, and decreases to 0.1 cm⁻¹ when the sample is heated to 20 K. The disappearance of the HCCCO IR signal and the decrease in that of CCCO, during the heating of the irradiated neon matrix suggest that during the sublimation of neon matrix at 20 K, dissociated H-atoms from c-C₃H₂O react with HCCCO and CCCO to form CH₂CCO and HCCCHO, the two isomers we have detected with the VUV irradiation of c-C₃H₂O ice at 10 K.

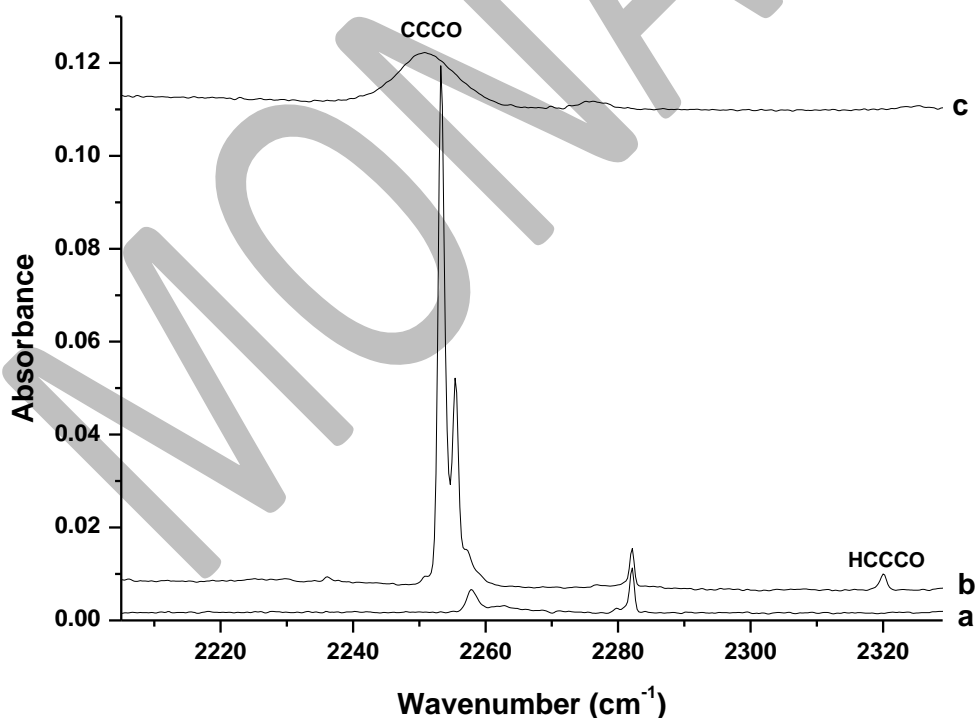


Figure 4: H-C=C=C=O and :C=C=C=O spectral region: IR spectrum of cyclopropenone (c-C₃H₂O) isolated in neon matrix at 3K, (a) before VUV irradiation, (b) After VUV irradiation, (c) After VUV irradiation followed by sublimation of neon atoms at 20 K, then a cooling down to 10 K to recover an irradiated c-C₃H₂O ice.

However, CCCO as precursor cannot be the only source of CH₂CCO and HCCCHO. Parts of CCCO trapped in neon matrix may also desorb during the sublimation of neon atoms without being involved in CCCO + 2H hydrogenation reaction. Others processes, such as radical-radical recombination or c-C₃H₂O photoisomerization, may occur during the photolysis of cyclopropanone and would certainly lead to CH₂CCO and HCCCHO. It is therefore interesting to analyze which photoproducts are detected under matrix isolation conditions and how they evolve during the sublimation of neon atoms at 20 K. Figure 5 shows the IR spectra of c-C₃H₂O isolated in Ne matrix at 3 K before and after VUV irradiation. Spectral regions have been selected, where IR signals of the photoproducts are clearly observed. Figure 5b shows that the main photoproducts detected in neon matrix at 3 K are CO, C₂H₂ and CCCO which have high IR signals in comparison with the IR signals of CH₂CCO and HCCCHO, formed in small quantities. However, in contrast with the CCCO IR signal, the CO and C₂H₂ absorption bands show structures due probably to interactions between CO and C₂H₂ fragments formed and trapped in the same neon cage (c-C₃H₂O → CO...C₂H₂).

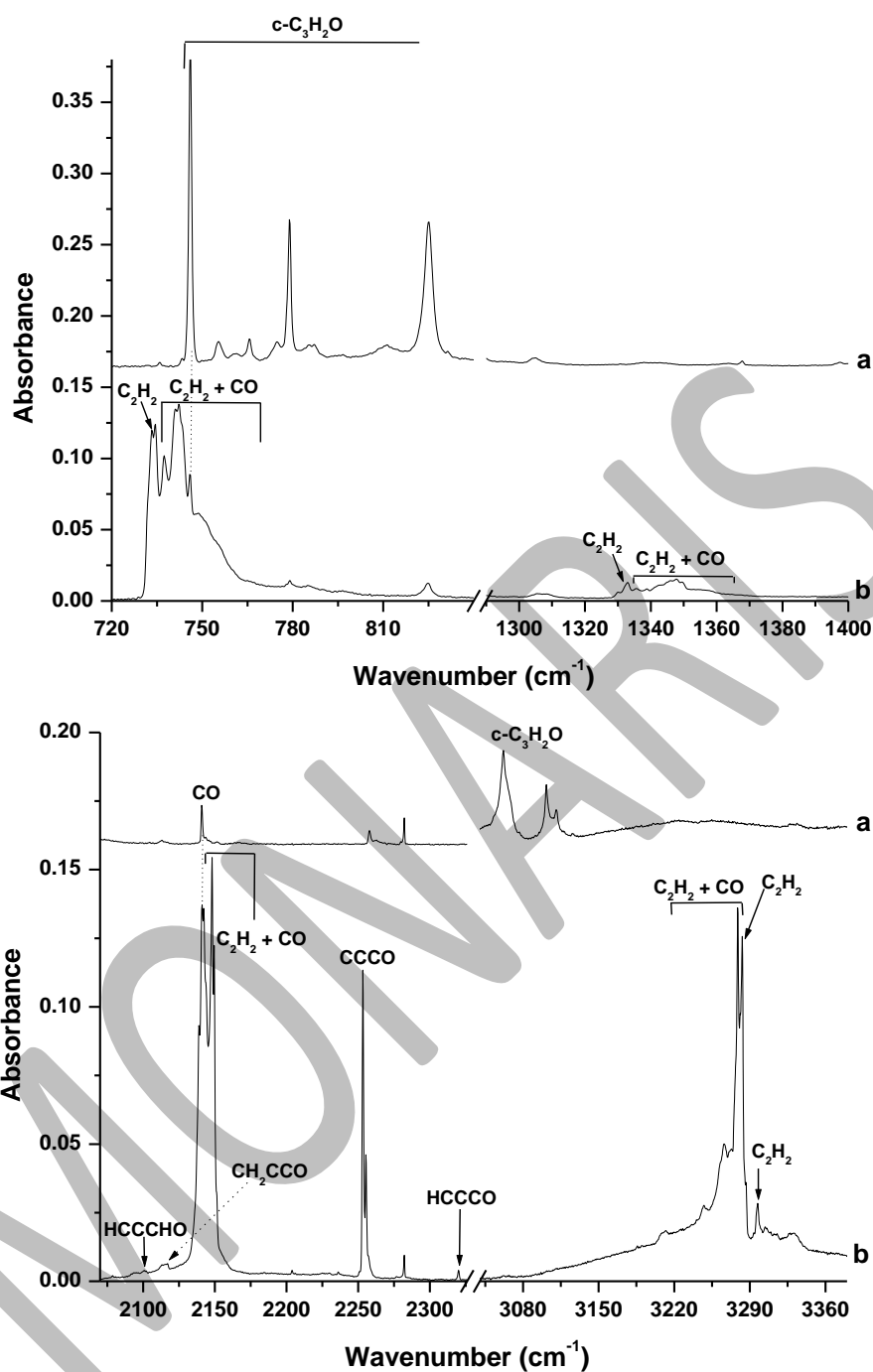


Figure 5: IR spectrum of c-C₃H₂O isolated in Ne matrix at 3 K: (a) before VUV irradiation, (b) after VUV irradiation.

Table 3 summarizes the new IR signals observed after VUV photolysis of c-C₃H₂O isolated in neon matrix and their assignments based from the literature data. Based on studies carried out by Zaslavov et al.⁹ on the isolation of C₂H₂:CO complex in argon matrix, we have identified 1:1 C₂H₂:CO complex isolated in neon matrix, through spectral complexation-induced shifts from CO and C₂H₂ absorption bands. Vibrational frequencies of 1:1 C₂H₂:CO complex are

marked with asterisks in table 3. The other IR signals observed around 733, 1332 and 3297 cm^{-1} on one the hand, and around 2140 cm^{-1} on the other characterize the two fragments trapped in the same neon cage, and probably due to $(\text{C}_2\text{H}_2)_m(\text{CO})_n$ aggregates ($m=1,2,3..$ and $n=1,2,3\dots$).

Table 3. Vibrational assignments of the main reaction products resulting from the VUV photolysis of cyclopropenone ($c\text{-C}_3\text{H}_2\text{O}$) isolated in Ne matrix.

IR signal After VUV photolysis (cm^{-1})	Assignments	Literature	(ref)
733.2	C_2H_2	732.2	(26)
734.4, 737.5*, 741.1, 742.5*, 748.9, 754.4	$(\text{C}_2\text{H}_2 + \text{CO})^\#$	742.5*, 747.4*	(9)
1332.2	C_2H_2	1329.9	(26)
1335.8, 1338.7, 1342.5, 1349.1, 1355.9	$(\text{C}_2\text{H}_2 + \text{CO})^\#$	-	
2100.9	HCCCHO	2107.3	(9)
2117.0	CH_2CCO	2125,0	(9)
2140.9	CO	2141.2	(27)
2139.3, 2144.1*, 2148.2, 2148.1, 2149.5	$(\text{C}_2\text{H}_2 + \text{CO})^\#$	2143.1*	(9)
2253.2	CCCO	2251.4	(9)
2320.0	HCCCO	2308.9	(21)
3283.1/3297.3	C_2H_2	3281.6/3295.1	(26)
3278.9, 3271.8, 3266.4, 3247.7, 3211.9	$(\text{C}_2\text{H}_2 + \text{CO})^\#$	3281.5	(9)

IR signals due to interactions between CO and C_2H_2 fragments formed and trapped in the same neon cage ($c\text{-C}_3\text{H}_2\text{O} \rightarrow \text{CO} \cdots \text{C}_2\text{H}_2$).

* Based on complexation-induced shifts predicted by the CCSD(T), wavenumbers marked with asterisks correspond to 1:1 $\text{C}_2\text{H}_2:\text{CO}$ complex isolated in neon matrix⁽⁹⁾.

The low IR signals of HCCCHO and CH_2CCO , detected at 2117.0 and 2100.9 cm^{-1} , suggests that the VUV photolysis of $c\text{-C}_3\text{H}_2\text{O}$ isolated in neon matrix leads mainly to photo fragmentation processes rather than direct photoisomerization into propynal and propadienone. As mentioned earlier, the total sublimation of neon matrix favors the CCCO + 2H reaction. We have calculated the integrated band intensities of CCCO, CH_2CCO and HCCCHO at 3 and 20 K. By increasing the sample temperature from 3 to 20 K, the integrated band intensity of CCCO decreases from 0.2 and 0.1 cm^{-1} , while that of CH_2CCO increases from 0.01 to 0.04 cm^{-1} and that of HCCCHO increases from 0.009 to 0.03 cm^{-1} . There are no data in the literature on the CCCO infrared band strength for estimating its column density.

However, we note that the column densities of propadienone and propynal at 3 K are 4.1×10^{14} and 5.6×10^{14} molecule. cm^{-2} and that they increase to reach 1.6×10^{15} and 1.9×10^{15} molecule. cm^{-2} at 20 K, respectively, due to CCCO hydrogenation. As mentioned above, parts of CCCO trapped in neon matrix may also desorb during the heating of the neon matrix.

This Infrared spectroscopy analysis part shows that the photolysis of cyclopropanone ($c\text{-C}_3\text{H}_2\text{O}$) in solid phase leads mainly to molecular conversion from the less stable isomer into the two most stable ones, propynal and propadienone, with abundances depending on the time of irradiations. The photolysis of cyclopropanone ($c\text{-C}_3\text{H}_2\text{O}$) leads also to fragmentation into CO and C_2H_2 and dehydrogenation to form tricarbon monoxide.

Photolysis of $c\text{-C}_3\text{H}_2\text{O}$: Mass spectrometry analysis

To complete this study, we have used the programmed thermal desorption coupled with mass spectrometry to confirm the formation of the reaction products. By investigating the mass spectrum of cyclopropanone ($c\text{-C}_3\text{H}_2\text{O}$) gas at room temperature, we show that mass fragments at $m/z = 54, 53, 52$ and 26 are detected with abundance distributions $d_{m/z} = 48\%, 12\%, 3\%$ and 100% , respectively.

Figure 6 (up) shows the TPD signals of cyclopropanone ($c\text{-C}_3\text{H}_2\text{O}$) ice without VUV photolysis, corresponding to the thermal desorption signals from mass fragments $m/z = 54, 53, 52$ and 26 . The distribution of the mass fragments shown in the TPD spectra are consistent with those deduced from the mass spectrum of cyclopropanone investigated at room temperature. The parent fragment of $c\text{-C}_3\text{H}_2\text{O}$ corresponding to $m/z = 54$ has a relative intensity of 48% , while the predominant fragment corresponding $m/z = 26$ has a relative intensity of 100% . The mass fragments at $m/z = 53, 52$ have abundance distributions $d_{m/z} = 12$ and 3% , respectively. Consequently, same $d_{m/z}$ abundance distributions are observed whatever the temperature of $c\text{-C}_3\text{H}_2\text{O}$ is. Even though at low temperature, we notice that amorphous cyclopropanone desorbs between 120 and 170 K, while the crystalline phase desorption occurs between 170 and 220 K. These desorption temperatures we measure under our experimental conditions are in good agreement with previous studies giving temperatures of $c\text{-C}_3\text{H}_2\text{O}$ ice desorption^{8,23} ranged between 150 and 230 K.

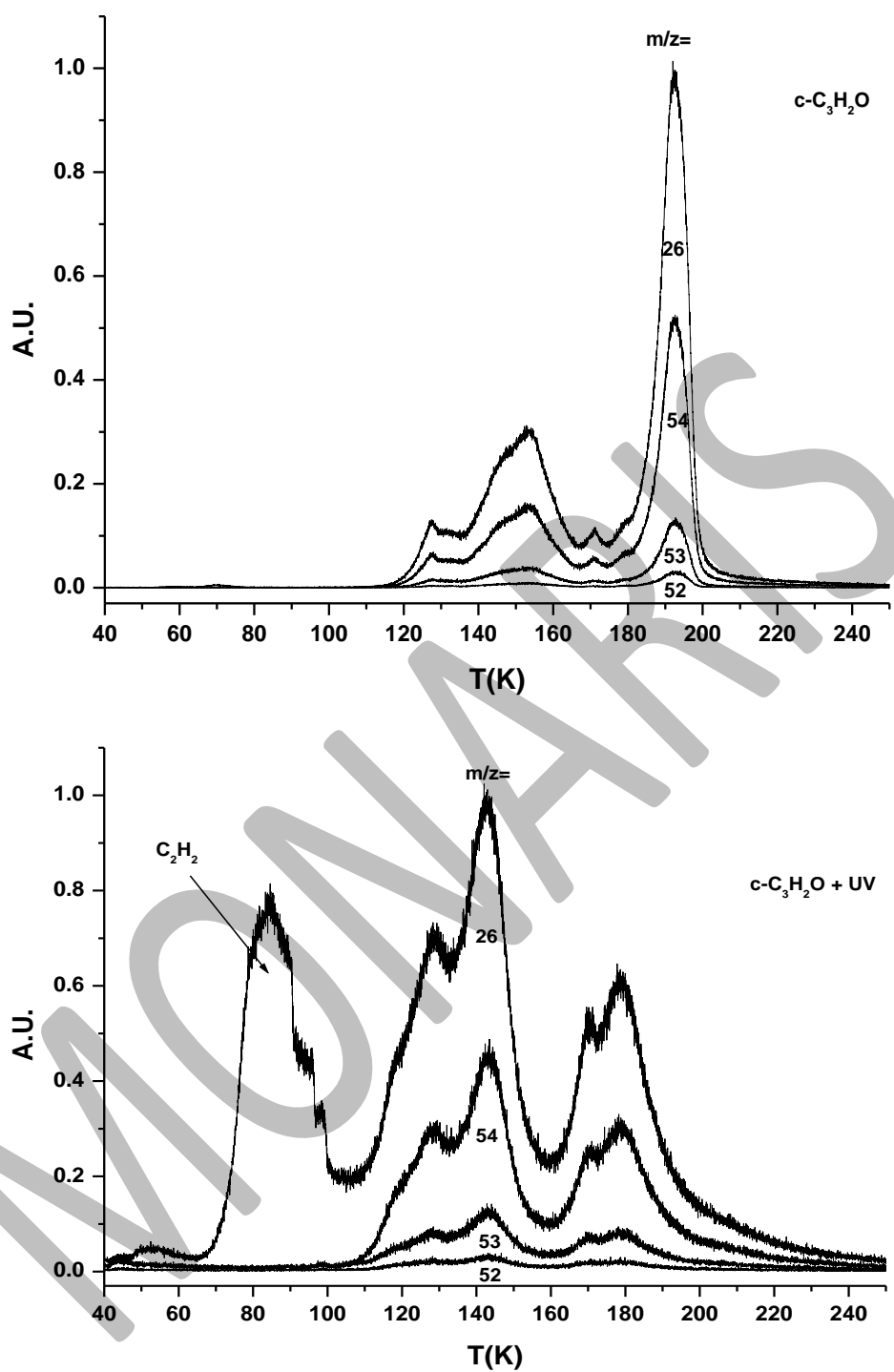


Figure 6: TPD spectra of cyclopropanone ($c\text{-C}_3\text{H}_2\text{O}$) ice formed at 10 K, without VUV photolysis (up) and after VUV irradiation (down).

However, after VUV photolysis of cyclopropanone ($c\text{-C}_3\text{H}_2\text{O}$) ice, the TPD signals of mass fragments at $m/z = 54, 53, 52$ and 26 shows behaviors completely different from those observed without photolysis. The signal corresponding to the mass fragment $m/z = 26$ which

appears at 65 K and reaches a maximum at 84K is consistent with desorption of C_2H_2 formed during the photolysis of $c-C_3H_2O$ and already discussed in the IR spectroscopy analysis section. While the signal due to the mass fragments at $m/z = 26$ corresponding to cyclopropenone starts appearing at 115K and disappears at 220K.

Cyclopropenone ($c-C_3H_2O$) and the two isomers formed after photolysis CH_2CCO and $HCCCHO$ have the same parent fragment at $m/z = 54$ and also the same fragment at $m/z = 53$ corresponding to the loss of one H-atom. However the three isomers have not the same desorption temperatures and mass fragment distributions $d_{m/z}$. The desorption temperature of cyclopropenone ($c-C_3H_2O$) is ranged between 120 and 220 K while that of propynal²⁸ is ranged between 125 and 155K. The abundance distribution $d_{m/z}$ of the mass fragments $m/z = 53$ and 54 are 12% and 48% for cyclopropenone and 100 % and 54% for propynal, respectively^{14,28}. Consequently, the ratios $d_{m/z=53}/d_{m/z=54}$ between the abundance distributions $d_{m/z}$ of the fragments at $m/z = 53$ and that of the fragments at $m/z = 54$ are 0.25 and 1.85 for cyclopropenone and propynal, respectively. Such a ratio, which can directly be measured as function of desorption temperatures during the thermal heating of $c-C_3H_2O$ ices with and without photolysis, may give information on potential desorption of the two other isomers of cyclopropenone. From the TPD signals corresponding to mass fragments $m/z = 54, 53$, Figure 7 shows the calculated ratios $d_{m/z=53}/d_{m/z=54}$ as a function of temperature during the thermal desorption of cyclopropenone ($c-C_3H_2O$). We show that without photolysis $d_{m/z=53}/d_{m/z=54}$ ratio is temperature independent and is approximately equal to 0.25, which is consistent with the abundance distributions $d_{m/z}$ of the fragments $m/z = 53$ and 54 from the mass spectrum of cyclopropenone whatever is the temperature. Upon thermal heating of irradiated cyclopropenone, we notice that $d_{m/z=53}/d_{m/z=54}$ ratio depends on the temperature between 150 and 175 K with a maximum at 160 K. It remains constant at temperatures ranged between 100 and 145 K and at temperatures higher than 180 K. Consequently, the two isomers of cyclopropenone formed during ice irradiation would desorb in the 150 - 175K temperatures range.

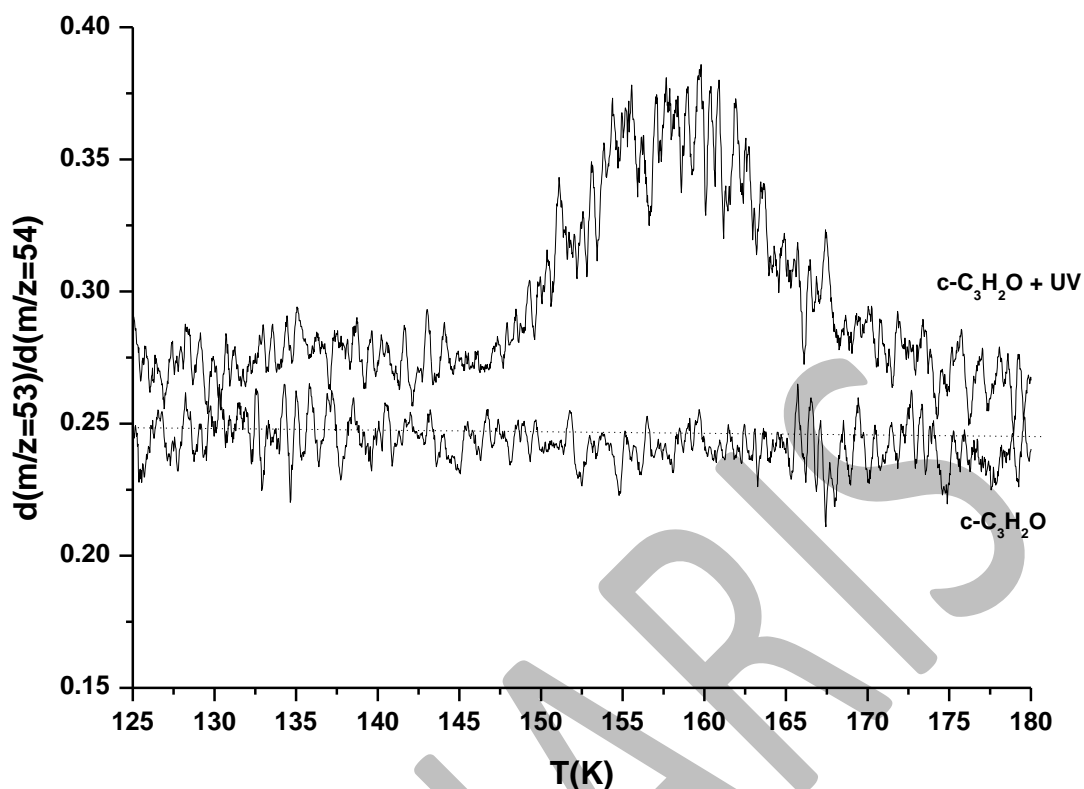
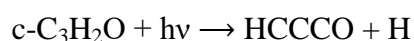
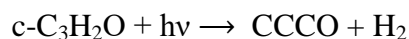
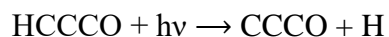


Figure 7: $d_{m/z=53}/d_{m/z=54}$ ratios between the abundance distributions $d_{m/z}$ of the fragments at $m/z = 53$ and 54 . Ratios calculated from TPD signals for the thermal desorption of cyclopropanone with and without VUV photolysis.

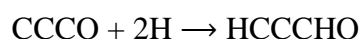
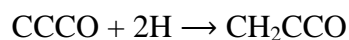
Discussion

Among the three isomers, $c\text{-C}_3\text{H}_2\text{O}$ (cyclopropanone), propynal (HCCCHO), and propadienone (H_2CCCO), we have investigated the VUV photolysis of the less stable one. We show through IR and mass spectrometry investigation that direct photolysis of $c\text{-C}_3\text{H}_2\text{O}$ ice at 10 K leads to C_2H_2 , CO , CH_2CCO and HCCCHO with abundance distributions depending on the time of irradiation. Additionally, C_3O has been detected through indirect photolysis of ice where cyclopropanone molecules isolated in neon matrix have been irradiated first. Then, the irradiated matrix is heated and cooled down to 10 K to recover an irradiated $c\text{-C}_3\text{H}_2\text{O}$ ice. The detection of CCCO through neon matrix isolation suggests that the irradiation of cyclopropanone leads to successive dehydrogenation process of $c\text{-C}_3\text{H}_2\text{O}$ to form CCCO .



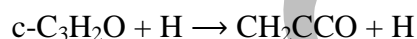


The absence of CCCO during the direct photolysis of c-C₃H₂O ice at 10K and the detection of HCCCHO and CH₂CCO isomers would suggest that the secondary reactions involving dissociated H-atoms and CCCO are very efficient in solid phase and lead to final stable products HCCCHO and CH₂CCO:



Consequently, the formation mechanism of the thermodynamically more stable isomers HCCCHO and CH₂CCO from the photolysis of the less stable one c-C₃H₂O is not a direct isomerisation photo-induced processing but it involves CCCO as reaction intermediate through CCCO + 2H addition reaction. Using DFT calculations²⁹, Shingledecker et al. showed that HCCCO + H reaction, to form CH₂CCO and HCCCHO, is expected to be barrierless and exothermic by 86.0 and 81.0 kcal mol⁻¹, respectively.

The dissociated H-atoms during c-C₃H₂O ice photolysis may also interact with c-C₃H₂O to form propynal and propadienone, through H-atom addition/abstraction reaction:



We have investigated recently the hydrogenation reaction of cyclopropenone¹⁴ ice at 10 K and shown that propynal (HCCCHO) and propadienone (CH₂CCO) are formed through H-atom addition/abstraction. HCCCHO is formed when the H-attack takes place on the carbon of the CO group to open the c-C₃H₂O ring which induces an H-abstraction from the C=C group. Propadienone (CH₂CCO) is produced when the H-addition occurs on one of the two carbons of the HC=CH group of c-C₃H₂O. The opening of the c-C₃H₂O ring is then followed by an H-abstraction from the central carbon of the chain to form CH₂CCO.

We notice that, all the products detected during the VUV photolysis c-C₃H₂O involve mechanisms already observed with UV photolysis (250-355 nm) of many carbonyl compounds. Photodissociation of formaldehyde and other carbonyls may occur through UV photolysis^{34,35} leading to dehydrogenation processes and the formation of CO. UV photolysis of cyclopropenone^{11,12} in aqueous and methanolic solutions leads to formation of CO and

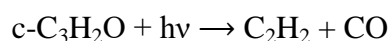
C_2H_2 . Photolysis of propynal³⁴ in the gas phase at 355 nm (3.5 eV) produces CO and C_2H_2 . In the present study, we use a VUV lamp with the main emission peak at 160 nm (7.7 eV) and a small additional peak at 125 nm (9.9 eV). The ionization potentials of cyclopropenone in gas phase are in the 9.57 - 16.1 eV range. Consequently, in addition to photolysis process which involves photons at 160 nm, ionization of cyclopropenone would be possible at 125 nm under our experimental conditions. The involvements of ionic reaction channels might then affect the set and distribution of photo-products. It is important to note that two similar studies have been carried out to describe the formation processes of propynal, cyclopropenone and propadienone from the photo-induced $C_2H_2 + CO$ reaction, using UV (4.3 and 5.6 eV)⁸ and X-ray (20 keV)^{9,10} photons. Zaslavskiy et al⁹ showed that 20 keV X-rays irradiation of $C_2H_2:CO$ complex isolated in an argon matrix yields C_3O , HC_3O , $HCCCHO$, H_2CCCO , and $c-H_2C_3O$, in addition to an unidentified intermediate product characterized, using IR spectroscopy, by a wide absorption band at 2265.6 cm^{-1} . This intermediate has been afterward assigned to at least three isomers of the $H_2C_3O^+$ cationic species. The same group¹⁰ reported theoretical and experimental study on the $H_2C_3O^+$ cations produced from 20 keV X-rays irradiation of $C_2H_2:CO$ complex. They showed that 20 keV X-rays irradiation of $C_2H_2:CO$ complex leads first to $HCCHCO^+$ cation which is more stable than $c-H_2C_3O^+$. Then, $HCCHCO^+$ is photo-rearranged into the most thermodynamically stable isomer H_2CCCO^+ . They suggest that $H_2C_3O^+$ cationic species should be the key intermediate in the formation of propynal, cyclopropenone, and propadienone through radiation-induced transformations of $C_2H_2:CO$ complex. However, J. Wang et al⁸ showed that propynal, cyclopropenone, and propadienone are also formed through UV Photolysis of CO- C_2H_2 ices using low photon energies ranged between 4.3 and 5.6 eV, without involvements of ionic reaction channels.

In the present study, using photons with energies ranged between 7.7 and 9.9 eV, the ionization effects could be quite limited, due probably to the fact that the photon energy at 125 nm is very close to the first ionization potential of cyclopropenone. On the other hand, no IR signal was detected around 2265 cm^{-1} , and which could be attributed to $H_2C_3O^+$ cation trapped in neon matrix. Under our experimental conditions, using ionizing radiation at 125 nm, cations may be generated in the neon matrix or ices by electron detachment from cyclopropenone but the cationic species cannot probably be experimentally detected due to the rapid electron-cation recombination.

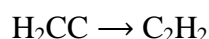
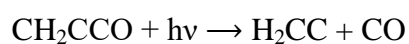
Based on previous theoretical studies^{30,31}, the relative binding energies of the three C_3H_2O isomers distribution shows (figure 8) that CH_2CCO is the most stable isomer, followed by

HCCCHO at $5.4 \text{ kcal mol}^{-1}$ and *c*-C₃H₂O at $10.8 \text{ kcal mol}^{-1}$. It is worth noting that propynal was observed in ISM in the cold cloud³² TMC-1 in 1988 (Irvine et al. 1988), but propadienone has not been detected in the ISM so far.

In addition to propynal and propadienone, carbon monoxide and acetylene are the two main reaction products observed after VUV photolysis of cyclopropenone through a reaction fragmentation:

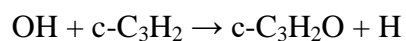
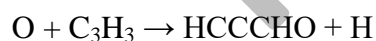


In this context, Ekern et al. performed ab initio studies^{6,33} of *c*-C₃H₂O potential surface showing that cyclopropenone transformation into C₂H₂ and CO requires energy input ranged between 43 and 48 kcal/mol. C₂H₂ and CO may also be produced as secondary reaction products from photodecomposition of primary photoproducts such as CH₂CCO through the following processing:

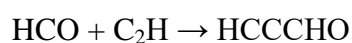
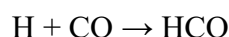
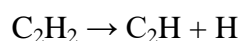
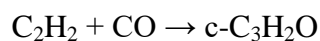


The dissociation²⁸ of CH₂CCO requires energy of 44.8 kcal/mol to yield vinylidene (H₂CC) and CO. The rearrangement of vinylidene^{28,29} to acetylene shows an energy barrier of 8.6 kcal/mol, which can be overcome under our experimental conditions. Photolysis of propynal³⁴ produces also CO and C₂H₂.

Three different mechanisms involving the formation of the three isomers of C₃H₂O have been investigated⁴ by Loison et al. They show that propadienone, propynal and cyclopropenone are formed through OH + 1-C₃H₂, O + C₃H₃ and OH + *c*-C₃H₂ reactions, respectively:



More recently, Wang et al⁸ showed by combining astrochemical modeling and experimental processing of C₂H₂-CO ices that cyclopropenone (*c*-C₃H₂O) and its isomer propynal (HCCCHO) are formed via reactions:



We show through the present study that, exposed to VUV irradiation, c-C₃H₂O lead to CO, C₂H₂ and CCCO photoproducts. Dissociated H-atoms released from the dehydrogenation of c-C₃H₂O would react with CCCO to form CH₂CCO and HCCCHO. It is worth to notice that the photolysis experiment we carried out in diluted phase at 3 K through neon matrix isolation has allowed isolating unstable reaction intermediates such as CCCO or HCCCO. However, even through neon matrix isolation, we did not detect intermediate photoproducts such as OH, HCO, 1-C₃H₂, c-C₃H₂ or C₃H₃. This shows that the photo-dissociation of c-C₃H₂O under our experimental conditions does involve many mechanisms discussed in previous astrochemical modeling.

Figure 8 summarizes the mechanisms of evolution of cyclopropenone (c-C₃H₂O) after VUV photolysis in solid phase: the formation of the two isomers from the barrierless and exothermic HCCCO + H reaction, the formation of c-C₃H₂O through c-C₃H₂ + O reaction and CO + C₂H₂ reactions. Based on previous ab initio calculations⁶, it is suggested that both reactions between c-C₃H₂ + O, c-C₃H₂ + O₂ and CO + C₂H₂ lead to cyclopropenone and while the reaction involving CO and C₂H₂ has high barrier energy of 48 kcal/mol, the one involving c-C₃H₂ and O₂ or c-C₃H₂ and singlet state of atomic oxygen have no energy barriers. These calculations are in good agreement with our experimental results due to the cage effects in the ices. In fact, c-C₃H₂O could be dissociated into (CO···C₂H₂) or (c-C₃H₂···O). The resulting fragments are formed and trapped in the same cages (c-C₃H₂O ↔ CO···C₂H₂) and (c-C₃H₂O ↔ c-C₃H₂ + O). Consequently, CO···C₂H₂ and c-C₃H₂···O rapid recombination, to form back c-C₃H₂O, are very probable. As there is a huge energy barrier between CO + C₂H₂ and c-C₃H₂O, the two photoproducts CO and C₂H₂ are stabilized at low temperature and could be observed experimentally. In an opposite side, when c-C₃H₂O is dissociated into (c-C₃H₂···O), the c-C₃H₂ + O recombination reaction has no energy barrier and would lead back to cyclopropenone.

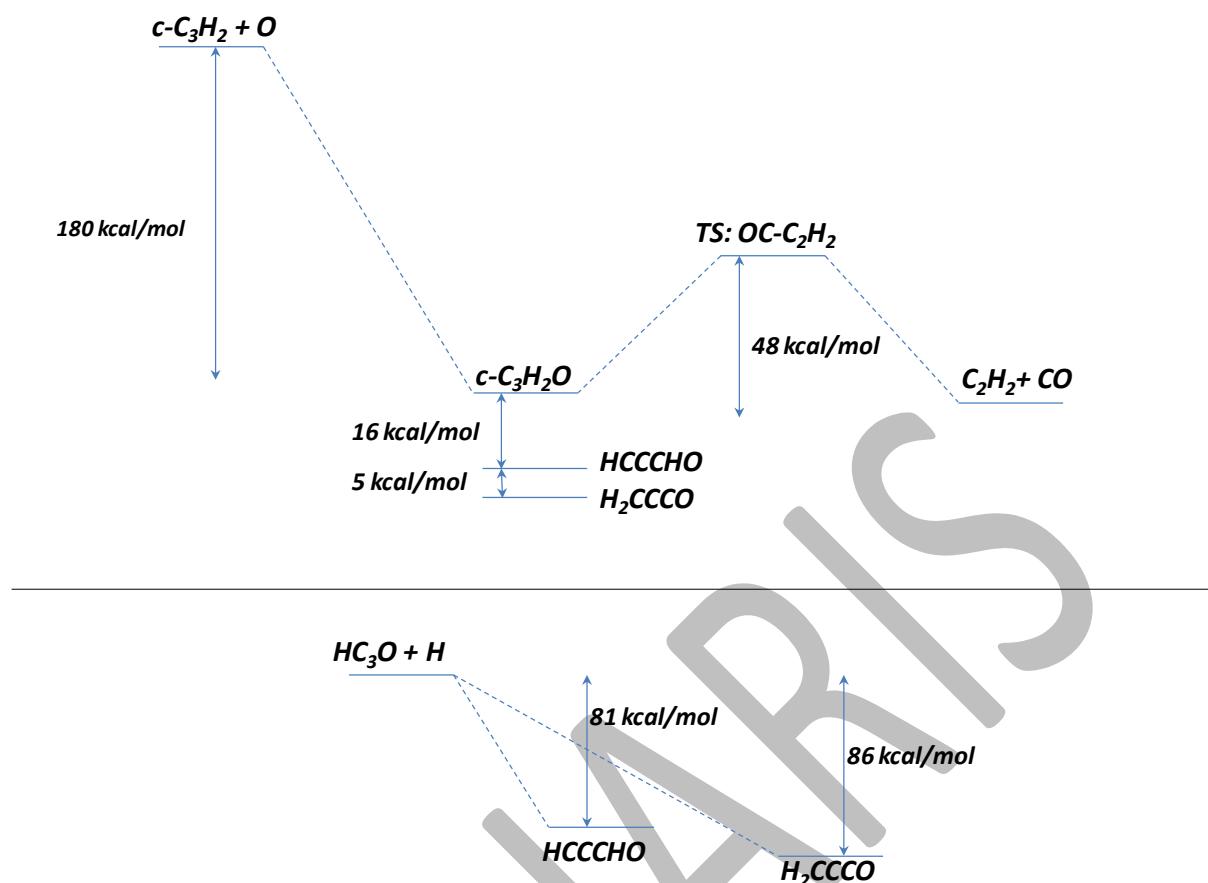


Figure 8: Mechanisms of evolution of cyclopropenone ($c\text{-C}_3\text{H}_2\text{O}$) through VUV photolysis. Relative binding energies of the three $\text{C}_3\text{H}_2\text{O}$ isomers and the relative energies of $\text{CO} + \text{C}_2\text{H}_2$, $c\text{-C}_3\text{H}_2 + \text{O}$, $\text{HC}_3\text{O} + \text{H}$ reactions are taken from Computational data^{6,29-31}. TS: $\text{OC-C}_2\text{H}_2$ is transition state. The energy diagram is not to scale.

In the interstellar medium, gas-phase and surface reactions on dust grains contribute to the formation of complex organic molecules such as cyclopropenone⁴ $c\text{-C}_3\text{H}_2\text{O}$. The reaction mechanisms leading to the production and consumption of neutral and ionic species, in the gas-phase and on grains, play an important role in the distributions and abundances of organic molecules in the interstellar medium. Icy objects in astrophysical environments undergo two main energetic processing, namely photolysis or photochemistry (using UV photons, without ionization processes) and radiation chemistry (using particles/ions bombardment and ionizing radiation), which may also produce low-energy (<20 eV) secondary electrons. These two main energetic treatments may involve in different formation pathways of complex organic molecules in the interstellar medium, although the dominant form of these two different energetic processing still to be clarified. Numerous experimental³⁶⁻³⁸ studies have shown that ion bombardment, ionizing radiation and UV photolysis have similar effects and lead to the same reaction products as they involve shared mechanism such as electronic excitation,

fragmentation, radical-radical recombination and radical-molecule reaction. In a context relevant to the present study, Zasimov et al¹⁰ shows that $C_2H_2 + CO$ reaction induced by 20 keV X-rays radiation yields C_3O , HC_3O , $HCCCHO$, H_2CCCO , $c\text{-}H_2C_3O$ and $H_2C_3O^+$. They show that $H_2C_3O^+$ cationic species is a reaction intermediate which involves in the molecular formation pathways of the neutral reaction products. However, J. Wang et al⁸ shows that the same reaction products are also formed through UV (4.3 - 5.6 eV) photolysis of $CO\text{-}C_2H_2$ ices, without involvements of ionic reaction channels. Still, the important difference between photolysis and radiation chemistry remains the depth of penetration³⁶, which is less important for photolysis processing. However, the use of VUV (7.7 – 9.9 eV) light, under our experimental conditions, may trigger more photochemistry than radiation chemistry and ionic reaction channels are probably very limited. We also showed that the dehydrogenation of $c\text{-}C_3H_2O$ under VUV irradiation is very efficient to form $CCCO$, $HCCCO$ and H-atoms trapped in neon matrix. H-atoms, in contrast to heavy species as O, may easily diffuse at low temperature during the heating of neon matrix to interact with $CCCO$ to form propadienone (CH_2CCO) and propynal ($HCCCHO$). Until today, only propynal³² and cyclopropenone², the two less stable isomers of propadienone have been detected in the interstellar medium. We show in the present study that, starting from the least stable isomer, the abundance of the $HCCCHO$ isomer is at best twice that of the most stable CH_2CCO isomer, if not equal. This suggests that CH_2CCO could be detectable in interstellar region where $HCCCHO$ and $CCCO$ are present.

Conclusion

We performed under interstellar conditions the VUV photolysis of $c\text{-}C_3H_2O$ in dilute phase and ice phase, monitored by FTIR spectroscopy and mass spectrometry. Our main results show that the VUV photolysis of cyclopropenone leads to the formation CO , C_2H_2 , and the two more stable isomers of cyclopropenone, namely propadienone (CH_2CCO) and propynal ($HCCCHO$). The photolysis of cyclopropenone in dilute phase allows the isolation of C_3O and $HCCCO$ as reaction intermediates which undergo to CH_2CCO and $HCCCHO$ through successive H-addition reactions. We also show that the distribution of these photoproducts depends on the irradiation time. At short irradiation time of 2 min, CO , C_2H_2 , CH_2CCO , $HCCCHO$ are formed with $CO:C_2H_2:CH_2CCO:HCCCHO$ column density ratio equal to 1:0.4:0.5:1, showing that CO and propynal, less stable than propadienone, are the predominant photoproducts with abundances twice those of C_2H_2 and CH_2CCO . By

increasing the irradiation time to 30 min, CO:C₂H₂:CH₂CCO:HCCCHO column density ratio is equal to 1:0.4:0.4:0.4, showing an equilibrium between the abundances of C₂H₂, CH₂CCO and HCCCHO, although CO remains the main photoproduct.

Data availability

The data of this paper will be shared on reasonable request to the corresponding author.

Conflicts of interest

There are no conflicts to declare.

MONARIS

References

1. H.-J. Wang, P. von Rague Schleyer, J. I. Wu, H.-J. Wang, *Int. J. Quantum Chem.*, 2011, 111,103
2. J. M. Hollis, A. J. Remijan, P. R. Jewell, F. J. Lovas, *ApJ*, 2006, 642, 933
3. T. Tokudome et al., in Kawabe R., Kuno N., Yamamoto S., eds, *ASP Conf. Ser, New Trends in Radio Astronomy in the ALMA Era: The 30th Anniversary of Nobeyama Radio Observatory*. Astron. Soc. Pac., San Francisco, 2013, 476p, 355
4. J.-C. Loison et al., *MNRAS*, 2016, 456, 4101
5. S. Petrie, *ApJ*, 1995, 454, L165
6. S. Ahmadvand, R. R. Zaari, A. V. Sergey, *ApJ*, 2014, 795, 173
7. L. Zhou, R. I. Kaiser, L. G. Gao, A. H. H. Chang, M.-C. Liang, Y. L. Yung, *ApJ*, 2008, 686, 1493
8. J. Wang, N. F. Kleimeier, R. N. Johnson, S. Gozem, M.J. Abplanalp, A. M. Turner, J. H. Marks., R. I. Kaiser, *PCCP*, 2022,24, 17449
9. P. V. Zasimov, S. V. Ryazantsev, D. A. Tyurin, V. I Feldman, *MNRAS*, 2021, 506, 3499
- 10 P.V. Zasimov, D. A. Tyurin, S.V. Ryazantsev, V. I. Feldman, *J. Am. Chem. Soc.*, 2022, 144, 8115
- 11 A. Poloukhine, P. V. Vladimir, *J. Org. Chem.*, 2003, 68, 7833
- 12 A. Poloukhine, V. V. Popik, *J. Org. Chem.*, 2003, 68, 783
- 13 W. R. Harshbarger, N. A. Kuebler, M. B. Robin, *J. Chem. Phys.*, 1974, 60, 345
14. M. Ibrahim, J-C. Guillemin, L. Krim, *MNRAS*, 2023, 524, 4037
15. L. Krim, M.Jonusas, J-L, Lemaire, G.Vidali, *PCCP*, 2018, 20, 1975
16. R. Breslow, J. Pecoraro, T. Sugimoto, *Organic Syntheses, Coll.*, 1988, 6, 361
17. J. Yang, K. McCann, J. Laane, *J. Mol. Struct.*, 2004, 695, 339
18. F. R. Brown, D. H. Finseth, F. A. Miller, K. H. Rhee, *J. Am. Chem. Soc.*, 1975, 97, 10
19. P. A. Gerakines, K. Ch. Materese, R.L. Hudson, *MNRAS*, 2023, 522, 3145
20. R.L. Hudson, R.F. Ferrante, M.H. Moore, *Icarus*, 2014, 228, 276
21. M. Jonusas, L. Krim, *MNRAS*, 2017, 470, 4564
22. R.L. Hudson, P.A. Gerakines, *MNRAS*, 2019, 482, 4009
23. C. J. Bennett, C. S. Jamieson, A. M. Mebel, R. I. Kaiser, *PCCP*, 2004, 6, 735
24. C. Gonzalez Diaz, H. Carrascosa, G. M. Muñoz Caro, M. A. Satorre, Y.-J. Chen, *MNRAS*, 2022, 517, 5744

25. Q. Jiang, W. R. M. Graham, *J. Chem. Phys.*, 1993, 98, 9251
26. M. Y. Lin, J. I. Lo, H. C. Lu, S. L. Chou, Y. C. Peng, B. M. Cheng, J. F. Ogilvie, 2014, *J. Phys. Chem. A*, 118, 3438
27. C. Pirim, L. Krim, *PCCP*, 2011, 13, 19454
28. M. J. Abplanalp, R. I. Kaiser, *PCCP*, 2019, 21, 16949
29. C.N. Shingledecker, S. Alvarez-Barcia, V. H. Korn, J. Kastner, *ApJ*, 2019, 878, 80
30. A. Karton, D. Talbi, *Chem. Phys.*, 2014, 436, 22
31. R. A. Loomis, B. A. McGuire, C. Shingledecker, C. H. Johnson, S. Blair, A. Robertson, A. J. Remijan, *ApJ*, 2015, 799, 34
32. W. M. Irvine, P. Friberg, A. Hjalmanson, et al., *ApJL*, 1988, 334, L107
33. S. Ekern, J. Szczepanski, M. Vala, *J. Phys. Chem.*, 1996, 100, 16109
34. G. Cheng, P. Ho, C. B. Moore, M. B. Zughul, *J. Phys. Chem.*, 1984, 88, 296
35. H.U. Zurcher, U. Bruhlmann, J. R. Huber, *Chem. Phys.*, 1982, 73, 403
36. P. A. Gerakines, M. H. Moore, R. L. Hudson, *J. Geophys. Res.*, 2001, 106, 381
37. C. Arumainayagam, R. Garrod, M. Boyer, et al. *Chem. Soc Rev.*, 2019, 48, 2293
38. E. Mullikin, C. Arumainayagam, et al. *ACS Earth Space Chem.*, 2018, 2, 863